

Field emission from short and stubby vertically aligned carbon nanotubes

M. Chhowalla,^{a)} C. Ducati, N. L. Rupesinghe, K. B. K. Teo,
and G. A. J. Amaratunga

Engineering Department, University of Cambridge, Trumpington Street, Cambridge CB2 1PZ,
United Kingdom

(Received 25 May 2001; accepted for publication 7 August 2001)

Electron emission from vertically aligned carbon nanotubes grown by plasma enhanced chemical vapor deposition has been measured using a parallel plate anode and a 1 μm tungsten probe. The field emission characteristics were measured as a function of the nanotube diameter, length, and areal density. It was found that less densely populated “short and stubby” nanotubes with diameters of 200 nm and heights of 0.7 μm showed the best emission characteristics with a threshold voltage of 2 V/ μm and saturation emission current density of 10 mA/cm². A triple junction between nanotube, substrate, and vacuum is proposed to explain our results. © 2001 American Institute of Physics. [DOI: 10.1063/1.1406557]

The excellent field emission characteristics of carbon nanotubes have been attributed to their high aspect ratio. It is believed that the longest vertically aligned carbon nanotubes with the smallest diameters, hence the largest electric field enhancement factor, are the most ideally suited for electron emission. Plasma enhanced chemical vapor deposition (PECVD) is a controllable and deterministic method for growing vertically aligned carbon nanotubes (VACNTs).^{1–5} The ability to control the location, orientation, and dimension of the nanotubes is essential for their use in microelectronics. Indeed, triode structures with a single nanotube inside 1 μm gates have been recently fabricated using direct current (dc)-PECVD.⁶

Several reports in the literature have obtained emission current densities ranging from 50 mA/cm² to 100 A/cm² at electric fields of 2–8 V/ μm for VACNTs using microscopic anodes.^{7,8} Such extraordinary emission characteristics along with their chemical inertness and mechanical robustness have led to speculation for their use as cathodes for microwave amplifiers and high power vacuum microelectronic switches. In these applications, patterning of the nanotubes is not necessary so long as high electron emission currents can be achieved. Therefore, high electron emission from “forests” of nanotubes is also of interest.

In this letter, we investigate the electron emission from VACNTs of varying lengths, diameters, and areal densities using a parallel plate configuration for macroscopic emission characteristics and a 1 μm tungsten anode for microscopic emission measurements from individual nanotubes. We show that dense forests of nanotubes exhibit relatively high threshold voltages (8–10 V/ μm) for electron emission due to electric field shielding effects. The most interesting result we obtain is that when the nanotubes’ height is further reduced so they have the appearance of being “short and stubby,” the threshold field decreases down to ~ 2 V/ μm and the emission current increases by almost an order of magnitude. The maximum saturation current density obtained using macroscopic anodes was 10 mA/cm². The emission currents obtained using the 1 μm tungsten anode ranged from 1 to 100

μA . The results appear to indicate that the high aspect ratio may not be the most important factor in obtaining the excellent electron emission characteristics.

The VACNTs were grown using dc-PECVD. The growth and material characteristics of the nanotubes deposited using this method are reported in detail elsewhere.⁹ Briefly, the VACNTs are grown at 700 °C onto Ni coated highly polished graphite substrates (1.5 cm \times 1.5 cm \times 1 mm) by initiating a dc glow discharge plasma of C₂H₂ and NH₃ (ratio = 75 sccm:200 sccm) at –600 V using an AE 1 kW dc generator. The nanotube diameter, length, and the areal density are dependent on the initial Ni film thickness, as can be seen in Fig. 1. In the parallel plate field emission measurement, the cathodes were 1.5 cm \times 1.5 cm \times 1 mm VACNTs and an evaporated Al film on a glass slide was used as the anode. By using a mask, anodes of several sizes could be evaporated and individually biased. The cathode and anode plates were separated by 100 μm high quality optical fibers. All the measurements were taken using a LabView controlled Keithley source/measure unit. The local field emission characteristics were measured using a tungsten tip having a radius of cur-

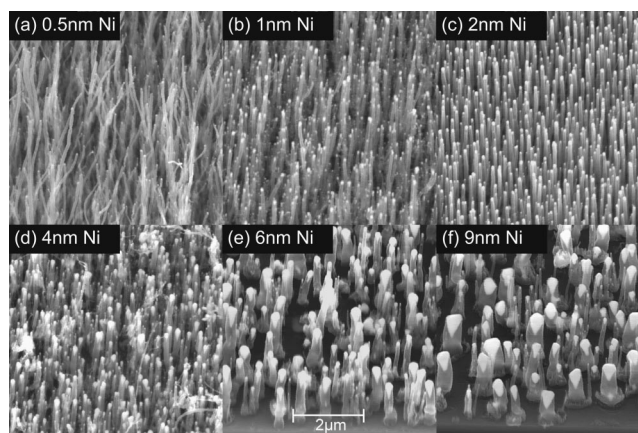


FIG. 1. Nanotube growth on varying initial Ni thicknesses. Note that the average diameter for the tubes grown on 0.5 nm Ni film is ~ 30 nm which increases to ~ 400 nm for tubes grown on 9 nm Ni films. The average tube height also decreases from ~ 8 to ~ 3 μm with Ni thickness. Furthermore the nanotube density decreases from $\sim 10^9$ to 10^8 cm⁻² for Ni films thicknesses ranging from 0.5 to 9 nm.

^{a)}Electronic mail: mc209@eng.cam.ac.uk

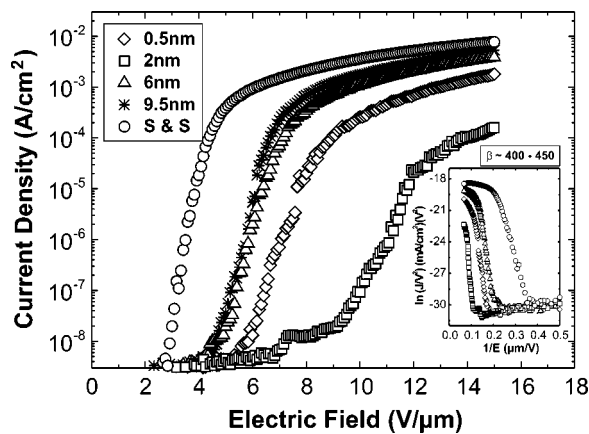


FIG. 2. (a) I - V emission characteristics measured in parallel plate configuration of the nanotubes shown in Fig. 1. The anode area was 0.5 cm^2 . The corresponding FN plots for each of the I - V curves are shown in the inset. The line in the FN plots was used to determine the calculated field enhancement factor (β). The curves labeled S & S correspond to the short and stubby nanotubes shown in Fig. 3.

vature of $1 \mu\text{m}$ observed in a scanning electron microscope (SEM). The anode to nanotube distance was determined by monitoring the current flow between the tip (biased to $+10 \text{ V}$) and cathode while gradually lowering it using a computer controlled piezo-electric stage. Vacuum of better than $1 \times 10^{-6} \text{ Torr}$ was achieved prior to initiating any measurements.

The field emission characteristics measured using the parallel plate configuration of the nanotubes is shown in Fig. 1 are plotted in Fig. 2. It can be seen that the most uniform and aligned nanotubes grown on 2 nm of Ni show the poorest emission characteristics in terms of having the highest turn on field (8 - $10 \text{ V}/\mu\text{m}$) as well as the lowest saturation current density ($0.1 \text{ mA}/\text{cm}^2$). This is attributed to the lack of field enhancement due to the close proximity and uniform height of the nanotubes, leading to the screening of the electric field. The very thin, long nanotubes grown on 0.5 nm Ni film show slightly better emission results with a turn on field of $\sim 6 \text{ V}/\mu\text{m}$ and a saturation current density of $\sim 1 \text{ mA}/\text{cm}^2$. These nanotubes are not entirely straight or as well ordered as those grown on 2 nm of Ni which introduces some nanotubes protruding above the rest, increasing their field enhancement factor and/or local bends in the tubes which may act as preferential emission sites due to defects.¹⁰ Finally, in Fig. 2 it can be seen that nanotubes grown on 6 and 9 nm of Ni film exhibit the best emission characteristics with a threshold field of $\sim 4 \text{ V}/\mu\text{m}$ and saturation current density of $5 \text{ mA}/\text{cm}^2$. The better emission from these nanotubes is likely to be a consequence of the decrease in the nanotube density by almost an order of magnitude. The corresponding Fowler-Nordheim (FN) plots are shown in the inset of Fig. 2. The field enhancement factor β , extracted from the linear region of the FN plots and assuming a work function of 5.0 eV for graphite, was found to be between 500 and 800 . Note that the geometrical β calculated (h/r) from the height (h) and radius (r) of the nanotubes is an order of magnitude (~ 50) lower than the FN β .

The influence of the geometrical β on the emission characteristics was further investigated by growing short and stubby nanotubes. These nanotubes, shown in Fig. 3, were grown on 6 nm of Ni film (in order to keep the same diam-

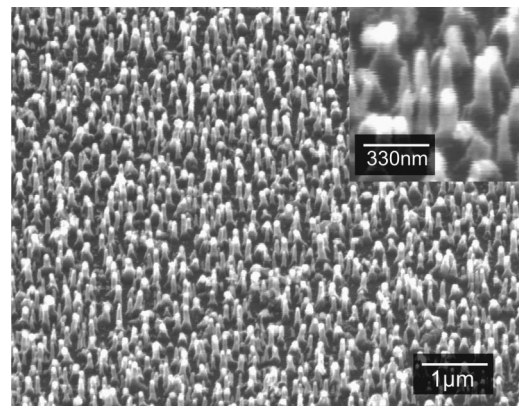


FIG. 3. SEM image of the short and stubby nanotubes. Note that the diameter and the areal density of these tubes are the same as those shown in Fig. 1. The overall deposition time was decreased by two thirds to reduce their overall height to $0.5 \mu\text{m}$.

eter and areal density as their longer counterparts shown in Fig. 1) for one third of the usual deposition time. The field emission curve from these short and stubby nanotubes measured in parallel plate geometry is shown in Fig. 2, labeled "S & S." Surprisingly, it can be seen that these tubes show the best emission characteristics with the lowest threshold field of $\sim 2 \text{ V}/\mu\text{m}$ and the highest saturation current density of almost $10 \text{ mA}/\text{cm}^2$. The corresponding FN plot is shown in Fig. 2(b) which gives a β of ~ 1200 , assuming a work function of 5.0 eV , significantly larger than the geometrical β (1 - 10).

The electron emission characteristics using a $1 \mu\text{m}$ tungsten probe were measured for the nanotubes in Fig. 1(f) and the short and stubby nanotubes. The field emission results are shown in Fig. 4. Comparable to the parallel plate measurements, the nanotubes grown on the 9 nm of Ni show a higher threshold field than the short and stubby tubes. However, the actual turn on field is slightly higher (6 - $8 \text{ V}/\mu\text{m}$) for the $1 \mu\text{m}$ probe measurements compared to parallel plate ones ($\sim 4 \text{ V}/\mu\text{m}$), indicating that in the parallel plate configuration where the electric field is present over a large area, some preferential emission occurs at low threshold voltages. In contrast, the short and stubby nanotubes show a lower threshold voltage of 2 - $4 \text{ V}/\mu\text{m}$, in agreement with the parallel plate measurements. The SEM observations of the short and stubby nanotubes show that they are fairly uniform, resembling a nanostructured thin film rather than individual

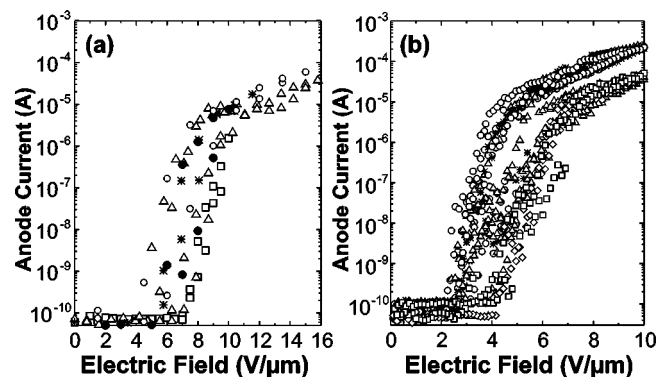


FIG. 4. Field emission using a $1 \mu\text{m}$ tungsten probe for (a) nanotubes grown on 9 nm of Ni film as shown in Fig. 1 and (b) short and stubby nanotubes as shown in Fig. 3.

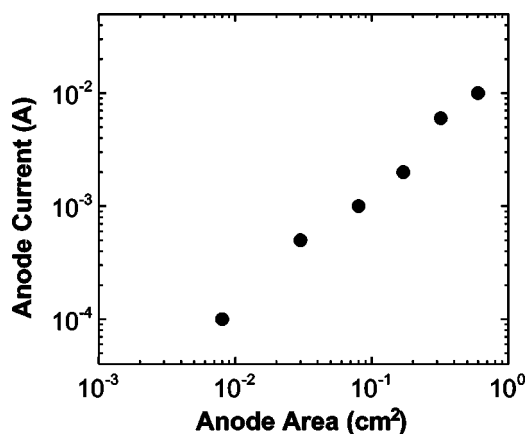


FIG. 5. Actual anode current vs the anode area.

nanotubes. Therefore, since the distributions in height and diameter amongst the short and stubby tubes are much smaller, the emission characteristics from macroscopic and microscopic anodes are expected to be similar.

The emission uniformity was investigated by monitoring the current as a function of the anode area, plotted in Fig. 5. It can be seen that, for macroscopic anodes, the emission current does indeed vary linearly with the area. Furthermore, for the 1 μm probe, the anode current is significantly higher than expected and does not correlate with the trend seen in Fig. 5. This indicates that the actual projected area from the 1 μm anode is likely to be much larger than its actual size. Also, since the nanotubes in this sample are in close proximity to one another, it is expected that electron emission from several tubes may contribute to the anode current even when a 1 μm probe is used. Nevertheless, the results of Fig. 5 confirm that the number of nanotubes contributing to the emission current increases as the anode area is increased and that isolated nanotubes are not solely responsible for the emission characteristics of nanotube “forests.”

Our results from the short and stubby nanotubes appear to indicate that shorter tubes with intermediate diameters may be the most suited for obtaining the best emission characteristics from forests of nanotubes. The large discrepancy between the calculated β from the FN plots and the geometrical β indicates that other mechanisms could be responsible for the electron emission process. The emission process need not only occur from the tip of the nanotubes. High field enhancement at the triple junction with the base of the nanotube, substrate, and vacuum could also cause the electrons to be emitted into the vacuum. Although the nanotubes for

these measurements were grown on graphite, our Auger and secondary ion mass spectroscopy measurements show the presence of hydrogenated amorphous carbon (*a*-C:H) on the surface¹¹ which is semiconducting and has an electron affinity that is different from that of graphite.¹² Therefore, a triple junction with infinitely large field enhancement can form between *a*-C:H, nanotubes, and vacuum. This process could also occur in longer nanotubes, but in a dense forest of tall nanotubes, the electron would most likely be trapped by a nearby nanotube, forcing the electron to be emitted via the nanotube tip. The exact emission process is presently being investigated by measuring the electron energy distributions, the results of which will be reported elsewhere.

In conclusion, we have found that forests of nanotubes with uniform height and diameter do not emit well due to screening effects. Field emission from short and stubby nanotubes (diameter of ~ 200 nm and height of ~ 0.5 μm) exhibit the lowest threshold field of 2 V/ μm and the highest saturation current density of 10 mA/cm². A triple junction between the substrate, nanotube, and vacuum may be responsible for the field emission from these nanotubes.

One of the authors (M.C.) wishes to thank VA Tech Reyrolle, another author (C.D.) acknowledges the CARBEN project, and a third author (K.B.K.T.) acknowledges the EC IST-FET Nanolith project and Association of Common Wealth Universities and the British Council.

¹W. Z. Li, S. S. Xie, L. X. Qian, B. H. Chang, B. S. Zou, W. Y. Zhou, R. A. Zhao, and G. Wang, *Science* **274**, 1701 (1996).

²Z. F. Ren, Z. P. Huang, J. W. Xu, J. H. Wang, P. Bush, M. P. Siegal, and P. N. Provencio, *Science* **282**, 1105 (1998).

³S. S. Fan, M. G. Chapline, N. R. Franklin, T. W. Tomblor, A. M. Cassell, and H. J. Dai, *Science* **283**, 512 (1999).

⁴C. Bower, O. Zhou, W. Zhu, D. J. Werder, and S. Jin, *Appl. Phys. Lett.* **77**, 2767 (2000).

⁵V. I. Merkulov, D. H. Lowndes, Y. Y. Wei, G. Eres, and E. Voelkl, *Appl. Phys. Lett.* **76**, 3555 (2000).

⁶M. A. Gillorn, M. L. Simpson, G. J. Bordanaro, V. I. Merkulov, L. R. Baylor, and D. H. Lowndes, *J. Vac. Sci. Technol. B* **19**, 573 (2001).

⁷W. Zhu, C. Bower, O. Zhou, G. Kochanski, and S. Jin, *Appl. Phys. Lett.* **75**, 873 (1999).

⁸V. I. Merkulov, D. H. Lowndes, and L. R. Baylor, *J. Appl. Phys.* **89**, 1933 (2001).

⁹M. Chhowalla, K. B. K. Teo, C. Ducati, N. L. Rupasinghe, and G. A. J. Amaratunga, A. C. Ferrari, D. Roy, J. Robertson, and W. I. Milne, *J. Appl. Phys.* (to be published).

¹⁰A. N. Obraztsov, A. P. Volkov, I. Y. Pavlovskii, A. L. Chuvilin, N. A. Rudina, and V. L. Kuznetsov, *JETP Lett.* **69**, 411 (1999).

¹¹K. B. K. Teo, M. Chhowalla, G. A. J. Amaratunga, W. I. Milne, D. G. Gasko, G. Pirio, P. Legagneaux, F. Wiczisk, and D. Pribat (unpublished).

¹²J. Schafer, J. Ristein, S. Miyazaki, and L. Ley, *J. Vac. Sci. Technol. A* **15**, 408 (1997).